



Pectin Based Graft Copolymer–ZnO Hybrid Nanocomposite for the Adsorptive Removal of Crystal Violet

Arun K. Kodoth¹ · Vishalakshi Badalamoole¹

Published online: 14 June 2019
© Springer Science+Business Media, LLC, part of Springer Nature 2019

Abstract

In this work we report the comparative study of the dye adsorption behavior of a Pectin-based terpolymer gel, pectin-*graft*-(poly(2-acrylamido-2-methyl-1-propane sulfonic acid)-*co*-acrylamide) (Pec-*g*-poy(AMPS-*co*-AAm)) and its nanocomposite with ZnO, (Pec-*g*-poy(AMPS-*co*-AAm)/ZnO) from aqueous solutions. Both the hydrogel systems have been synthesized using microwave irradiation technique through free radical polymerization. Swelling behavior of the systems was studied in buffer solutions of pH ranging from 1.2 to 13 and maximum swelling was observed in neutral medium. The equilibrium swelling of parent gel was found to be 28.12 g/g whereas it was 16.54 in the case of nanocomposite. Cationic dye, crystal violet, is employed to assess the adsorption efficiency of the gel samples from aqueous solutions. The influence of initial dye concentration was investigated. A maximum adsorption of 329 and 568 mg/g has been observed for the parent gel and the nanocomposite respectively. The presence of ZnO is observed to enhance the adsorption capacity of Pec-*g*-poy(AMPS-*co*-AAm) gel considerably. The kinetic studies revealed a second order adsorption process with high rate of initial adsorption in the case of the nanocomposite when compared to the parent gel and the isotherm studies reveals that the adsorption process fits well into Langmuir model. The evaluation of thermodynamic parameters indicated the adsorption process to be exothermic and spontaneous. Desorption studies under acidic condition showed that almost 96% of the adsorbed dye molecules could be desorbed to the stripping solution of pH 1.2 which support the use of these hydrogel systems for the repeated use as adsorbents for cationic dyes.

Keywords Pectin · ZnO nanoparticles · Microwave · Nanocomposite · Dye adsorption

Introduction

Synthetic dyes have been extensively used in industries such as textile, printing and dyeing, leather, cosmetic, petroleum, etc. [1]. These dyes are present in the effluents which are discarded by the industries and they can cause major damage to the ecosystem [2–5]. Most of these compounds cause depletion of oxygen content of water and will adversely affect aquatic life. In addition to this, several dyes and their decomposition products exhibit carcinogenic as well as mutagenic

effects [6–8]. Removal of these dyes from effluents can be carried through various methods out of which adsorption is the most widely used method due to its simplicity, low cost and effectiveness [9–12].

A wide variety of systems have been reported as adsorbents for the dye removal. Among these systems, stimuli responsive hydrogels and nanocomposites play a major role in water purification due to their improved physical and chemical properties [13]. k-Carrageenan coated super paramagnetic nanoparticles [10], cellulose nanocrystal nanocomposite hydrogels [14], clay nanocomposite [15, 16], kaolin composite hydrogel [17], agricultural waste [18], metal–organic frameworks [19], amyloid fibrils [20], straw-based adsorbent [21] etc. are some of these systems. Among these, nanocomposite hydrogels have got much attention due their high adsorption capacity and ease of preparation [22]. Ghaedi et al. [23] synthesized zinc oxide nanoparticles loaded activated carbon and evaluated its adsorption capacity towards malachite green. Zhang et al. [24] synthesized

Electronic supplementary material The online version of this article (<https://doi.org/10.1007/s10924-019-01488-x>) contains supplementary material, which is available to authorized users.

✉ Vishalakshi Badalamoole
vishalakshi2009@yahoo.com

¹ Department of Post-Graduate Studies & Research in Chemistry, Mangalore University, Mangalagangothri, DK, Karnataka 574199, India

ZnO-layered double hydroxide @ graphitic carbon nitride composite for the consecutive adsorption and photodegradation of cationic dyes under UV and visible lights and 90% adsorption was achieved in five cycles. Zhang et al. [25] reported the synthesis of citrus pectin-derived carbon microspheres against the adsorption of methylene blue. The system has been synthesized via facile hydrothermal method where the microspheres showed good adsorption capacity and reusability too. Pectin-cerium (IV) tungstate nanocomposite [26] has been found to be very useful for the adsorptive removal of methylene blue from aqueous solutions. Pectin thorium(IV) tungstomolybdate nanocomposite [27] has been used for the removal of both the heavy metal ions and the cationic dye malachite green. Singha et al. [28] formulated a novel IPN system, pectin-*g*-(sodium acrylate-*co*-*N*-isopropylacrylamide) for the synergistic removal of cationic dyes such as methyl violet, methylene blue and methyl orange as well as toxic bivalent metal ions. The optimum conditions for the adsorption process have been derived and thermodynamically feasible chemisorptions were observed throughout. Sharma et al. [29] reported the modification of *Hibiscus cannabinus* fiber with acrylic acid and a binary mixture of acrylic acid and acrylamide for the adsorptive removal of methylene blue from aqueous solutions.

Pectin is a valuable byproduct extracted from fruit waste. It is present in all higher plants as polysaccharide with partially esterified polygalacturonic acid [30]. Its binding ability with many organic and inorganic materials makes it useful for the preparation of adsorbent materials [31]. It is rich with functional groups such as carboxyl–carboxylate and hydroxyls, which can actively participate in cationic dye removal [32]. But the low mechanical stability is the major drawback of pectin based hydrogels which is one of the key parameters in adsorption processes [33]. 2-Acrylamido-2-methyl-1-propanesulfonic acid (AMPS) has received much attention since it has strongly ionizable sulfonate group which will supply anionic sites for the adsorption process [34]. In recent years, polyacrylamide (PAAm) containing hydrogels have become the most acceptable adsorption materials in wastewater treatments due its binding capacity with dyes and it provides mechanical strength to the hydrogels. The amide ($-\text{CONH}_2$) groups in PAAm can act as active sites to remove soluble ions from water by coordination and chelation [14]. The unique property of nanoparticles is the surface area, which helps in adsorption of materials. Zinc oxide nanoparticles have been widely used for the adsorption of organic dyes in native form [24, 35–37] or as a combination with synthetic polymer [38] or polysaccharide [39–41] or inorganic salts [42]. Addition of zinc oxide to the polymeric systems provides additional sites for the adsorption process.

The present work is undertaken to develop a pectin based adsorbent material with improved mechanical strength and good adsorption efficiency for cationic dyes. A terpolymer

gel has been made by graft copolymerization of AMPS and AAm in the presence of *N,N'*-methylene-bis-acrylamide (MBA) on pectin. A nanocomposite of this gel has also been made by the incorporation of ZnO nanoparticles into the gel network. The parent pectin-graft-copolymer gel and the nanocomposite have been evaluated for their ability to adsorb cationic dye, crystal violet (CV) from aqueous solutions.

Experimental Section

Materials

All the chemicals used for the experiments were of analytical reagent grade. Pectin from citrus peel (Pec) and 2-acrylamido-2-methyl-1-propanesulfonic acid (AMPS) were obtained from Sigma Aldrich Chemical Company, India. Acrylamide (AAm) and sodium hydroxide were obtained from Loba Chemie, India. *N,N'*-methylene-bis-acrylamide (MBA), ammonium peroxodisulphate (APS) and acetone were obtained from Spectrochem Pvt. Ltd., Mumbai, India. Zinc sulfate was obtained from Thermo Fisher Scientific India Pvt. Ltd., India. The dye, 'Crystal Violet' (CV) with purity of 96% was obtained from Rankem, RFCL Ltd., Delhi, India. All the chemicals were used without further purification. Double distilled water was used throughout the experiments.

Methods

Synthesis of Zinc Oxide (ZnO) Nanoparticles

ZnO nanoparticles were synthesized as reported earlier [43]. To the aqueous zinc sulfate solution, aqueous sodium hydroxide was added drop wise in a molar ratio 1:2 under stirring at room temperature. The stirring was continued for 12 h. The resulting solution was then filtered and the precipitate obtained was washed with deionized water, and dried in a hot air oven at 100 °C for 12 h.

Microwave Assisted Synthesis of Pectin-graft-(poly(2-acrylamido-2-methyl-1-propanesulfonic acid)-*co*-polyacrylamide) [Pec-*g*-poy(AMPS-*co*-AAm)] and [Pec-*g*-poy(AMPS-*co*-AAm)/ZnO]

Synthesis of the nanocomposite hydrogel system has been carried out as reported in our previous works [44–46]. In brief, a mass of 0.5 g pectin was added to 15 mL water and stirred overnight to get a homogeneous solution. Homogeneous dispersion of ZnO in pectin solution was achieved by adding 0.002 g ZnO (0.025 mmol) followed by sonication for 15 min. To this solution, the monomers, AMPS (0.15 g;

0.724 mmol) and AAm (0.4 g; 5.627 mmol) were added and stirred. Added 0.015 g (0.066 mmol) APS as initiator and 0.015 g (0.097 mmol) MBA as cross linking agent and continued stirring for 3 h. Microwave was then passed through the mixture for 25 s at a power of 80 W. The obtained gel was then purified in acetone and dried at 50 °C. The P-g-(PAMPS-co-PAAm) gel was also made without the addition of ZnO following the same procedure as above.

Fourier Transform Infrared Spectroscopy (FTIR)

FTIR spectra of Pec-g-poy(AMPS-co-AAm) and Pec-g-poy(AMPS-co-AAm)/ZnO were recorded on a FTIR spectrometer (Shimadzu IR Prestige 21, Japan) in transmittance mode in the range of 500 cm⁻¹ to 4000 cm⁻¹.

Thermogravimetric Analysis (TGA)

TGA of Pec-g-poy(AMPS-co-AAm) and Pec-g-poy(AMPS-co-AAm)/ZnO were recorded on the thermogravimetric analyzer SDT Q600 V20.9 (Japan). The samples were heated from room temperature to 700 °C under nitrogen atmosphere at a rate of 10 °C/min.

X-ray Diffraction (XRD)

Powder X-ray diffraction pattern of Pectin, ZnO and Pec-g-poy(AMPS-co-AAm)/ZnO were recorded using Benchtop X-ray diffractometer, Rigaku MiniFlex 600 (Japan). The diffraction patterns were recorded at an angle range of 0° to 80° at room temperature at an analysis rate of 2°/min.

Field Emission Scanning Electron Microscopy (FESEM) and Energy Dispersive X-ray Spectroscopy (EDS)

Morphological study of Pec-g-poy(AMPS-co-AAm) and Pec-g-poy(AMPS-co-AAm)/ZnO and the dye adsorbed Pec-g-poy(AMPS-co-AAm)/ZnO was carried out by recording the FESEM images using JEOL-JSM5800LV (Japan) Scanning electron microscope. The micrographs were recorded with different magnifications.

High Resolution Transmission Electron Microscopy (HRTEM)

The size and shape of the nanoparticles in the Pec-g-poy(AMPS-co-AAm)/ZnO were checked using JEOL/JEM 2100 transmission electron microscope (USA) operating at 200 kV.

Swelling Studies

The swelling behaviour of Pec-g-poy(AMPS-co-AAm) and Pec-g-poy(AMPS-co-AAm)/ZnO were investigated in buffer

solutions of pH ranging from 1.2 to 13.0 at room temperature. Shimadzu AUX120 (Japan) electronic weighing balance was used for the weight measurements with an accuracy of ±0.1 mg. Pre-weighed parent gel and nanocomposite gel samples were immersed in excess of the buffer solutions. After specific time intervals, the samples were taken out and the surface adhered liquid droplets were removed with blotting paper. The increases in weight of the samples were recorded. The measurements were made till the weight of the swollen gel attained a constant value. Swelling experiments were repeated three times and average values were considered. The swelling ratio, SR (g/g) was calculated using the following equation

$$SR = \frac{W_t - W_0}{W_0} \quad (1)$$

where W_0 and W_t are the weights of the sample in dry state and swollen state at time t respectively.

Dye Adsorption and Desorption Studies

In order to estimate the dye adsorption capacity of the parent gel and the nanocomposite gel, 12 ± 2 mg of gel samples were suspended in aqueous dye solutions of concentrations varying in the range 20–400 ppm. The samples were allowed to equilibrate for 7 h at room temperature. The dye solutions were decanted after the specified time period and the amount of unabsorbed dye in the solution was measured using a UV–Vis spectrophotometer (Shimadzu UV-160A) at the wavelength of 588 nm. The equilibrium adsorption capacity of the gels, Q_e (mg/g), was calculated according to the following equation

$$Q_e = (C_0 - C_e) \times \frac{V}{m} \quad (2)$$

where C_0 is the initial dye concentration (mg/L), C_e is the residual dye concentration at equilibrium (mg/L), V is the volume of solution (L) and m is the amount (g) of dry gel samples used for adsorption studies.

To check the re-usability of the gel systems as adsorbents, the desorption experiments were carried out in pH 1.2 solutions (prepared using HCl). About 12.0 mg each of the gel samples were suspended in dye solutions separately for 7 h. The samples were then removed, washed with water and dried. They were kept immersed in pH 1.2 solutions for 2 h at room temperature. Aliquot of the solutions were then analyzed using UV–Vis spectrophotometer and the amount of dye desorbed was calculated. The percentage of desorption (D) was calculated using the following equation,

$$D(\%) = \frac{\text{Amount of dye molecules desorbed (mg)}}{\text{Amount dye molecules adsorbed (mg)}} \times 100 \quad (3)$$

Results and Discussion

Synthesis of Pec-g-poy(AMPS-co-AAm) and Pec-g-poy(AMPS-co-AAm)/ZnO by Microwave Irradiation Method

Under the influence of microwave dielectric heating, the generation of free radicals from the initiators facilitates the formation of radical sites on pectin along with the formation of copolymer chains containing AMPS and AAm. These copolymer chains are grafted to the pectin backbone. Crosslinking of the grafted copolymer chains are brought about by the addition of the crosslinking agent MBA. This results in the formation of a network like structure. In the case of the nanocomposite hydrogel, the ZnO nanoparticles occupy the free space within the network system. Mechanism of formation of Pec-g-poy(AMPS-co-AAm)/ZnO is shown in Fig. 1.

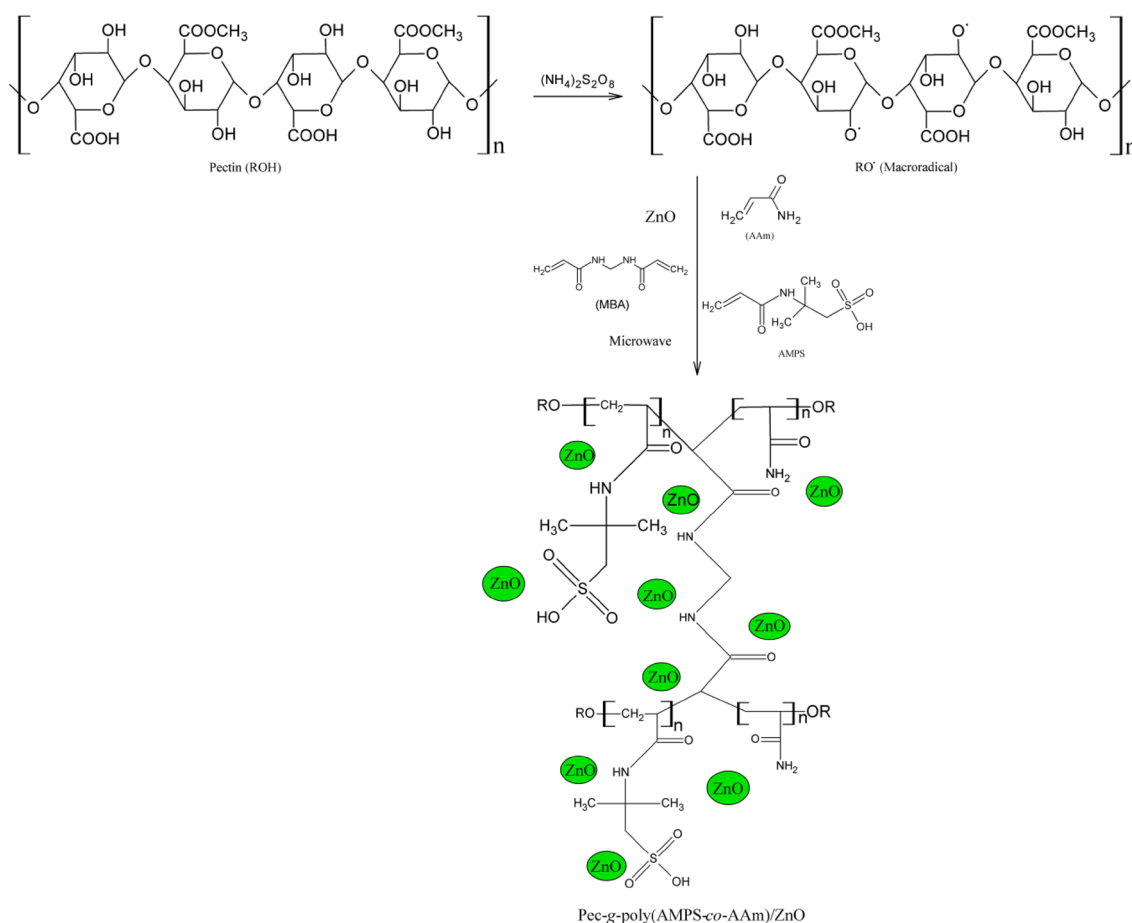


Fig. 1 Mechanism of formation of Pec-g-poly(AMPS-co-AAm)/ZnO

FTIR Spectroscopy

The FTIR spectra of Pec-g-poy(AMPS-co-AAm) and Pec-g-poy(AMPS-co-AAm)/ZnO are displayed in Fig. 2. Bands in the range of $3250\text{--}3500\text{ cm}^{-1}$ are due to the --OH and NH stretching present in pectin and acrylamide respectively. The broadening of band is attributed to the intermolecular hydrogen bonding [47]. The band at 1685 cm^{-1} is attributed to the C=O stretching of pectin. The S=O stretching of AMPS occurs at 1040 cm^{-1} . The additional bands at 670 cm^{-1} and 555 cm^{-1} in the case of the nanocomposite hydrogel Pec-g-poy(AMPS-co-AAm)/ZnO (Fig. 2b) are due to the stretching vibrations of Zn--O bonds.

Thermogravimetric Analysis

The thermogravimetric analysis of the parent gel and its nanocomposite are displayed in Fig. 3. Both the samples show three step degradation. The first stage of weight loss for Pec-g-poy(AMPS-co-AAm) (Fig. 3a) occurs from 25 to $197\text{ }^\circ\text{C}$ which is attributed to the loss of water molecule from the sample. The second step starting at

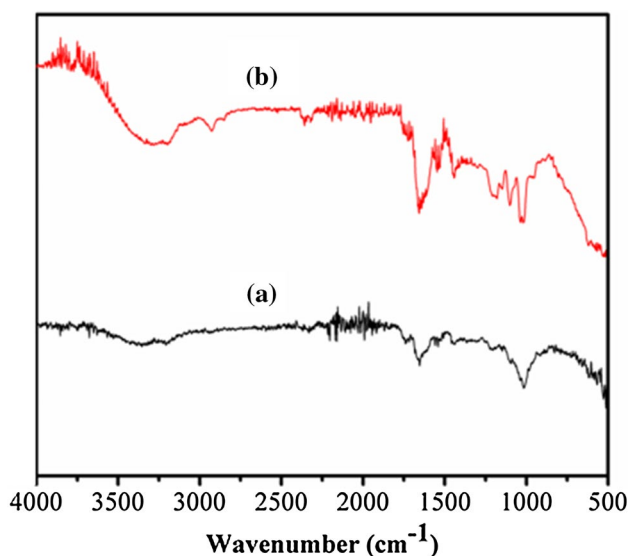


Fig. 2 FTIR spectra of **a** Pec-g-poly(AMPS-co-AAm) and **b** Pec-g-poly(AMPS-co-AAm)/ZnO

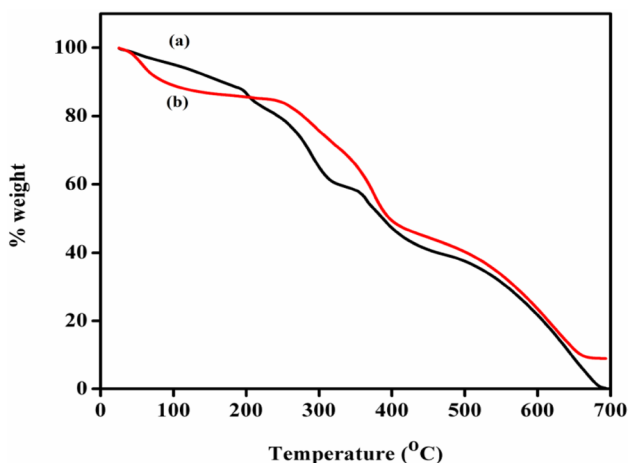


Fig. 3 Thermograms of **a** Pec-g-poly(AMPS-co-AAm) and **b** Pec-g-poly(AMPS-co-AAm)/ZnO

a temperature of 240 °C is due to the decomposition of polysaccharide backbone. The third and last degradation occurs in the range 400–670 °C. Complete degradation of the system can be observed at 670 °C. For the nanocomposite sample, Pec-g-poly(AMPS-co-AAm)/ZnO the first stage of weight loss occurs from 25 to 100 °C which is due to dehydration. The second stage marking degradation of polymer backbone starts at 250 °C and extends till 400 °C. The third stage extends from 400 to 670 °C. At 670 °C, a mass of around 8.6% remains confirming the presence of ZnO nanoparticles.

XRD Analysis

Figure 4 displays the XRD pattern of Pec-g-poly(AMPS-co-AAm), ZnO and Pec-g-poly(AMPS-co-AAm)/ZnO. The amorphous nature of Pec-g-poly(AMPS-co-AAm) can be concluded from the broad XRD pattern (Fig. 4a) occurring at lower 2θ values. The sharp crystalline peaks of ZnO nanoparticles (Fig. 4b) can be observed at 2θ values 31.8, 34.4, 36.2, 47.5, 56.5, 62.8, 66.4°, 68.1 and 68.9°. The nanocomposite hydrogel (Fig. 4c) shows crystalline nature due to the presence of highly crystalline ZnO nanoparticles. The crystalline peaks are observed almost at the same 2θ value as that of ZnO nanoparticles which confirms the dispersion of ZnO nanoparticles within the graft copolymer network.

FESEM and EDS Analysis

Under the scanning electron microscope, the surface of the gel Pec-g-poly(AMPS-co-AAm) (Fig. 5a) appears to be rough, layered and heterogeneous. The surface of the grafted copolymer gel appears to be continuous and uneven. The nanocomposite, Pec-g-poly(AMPS-co-AAm)/ZnO (Fig. 5b) shows a smooth surface with the uniform distribution of ZnO nanoparticles throughout the system. On adsorption of the dye, the surface of the nanocomposite is found to be saturated with uniform dispersion of dye molecules (Fig. 5c).

The elemental composition of Pec-g-poly(AMPS-co-AAm) and Pec-g-poly(AMPS-co-AAm)/ZnO was assayed using EDS analysis (Fig. 6a) in combination with the FESEM analysis to confirm grafting and nanocomposite formation. EDS spectrum of Pec-g-poly(AMPS-co-AAm) indicated the presence of carbon, oxygen, nitrogen and sulfur which confirmed grafting. The additional peak of Zn was observed in the EDS spectra of Pec-g-poly(AMPS-co-AAm)/ZnO (Fig. 6b) along with the peaks for C, O, N and S.

TEM Analysis

High resolution TEM analysis of the nanocomposite gel, Pec-g-poly(AMPS-co-AAm)/ZnO indicates the spherical nature of the ZnO nanoparticles embedded within the hydrogel network system (Fig. 7a–c). The electron diffraction from a selected area (SAED) of the sample is displayed in Fig. 7d. The bright concentric rings indicate the presence of well crystallized ZnO nanoparticles with hexagonal wurtzite structure. These rings matches with the peaks in XRD pattern which confirms the crystallinity of the nanocomposite and structure of the nanoparticles incorporated in the gel network [48].

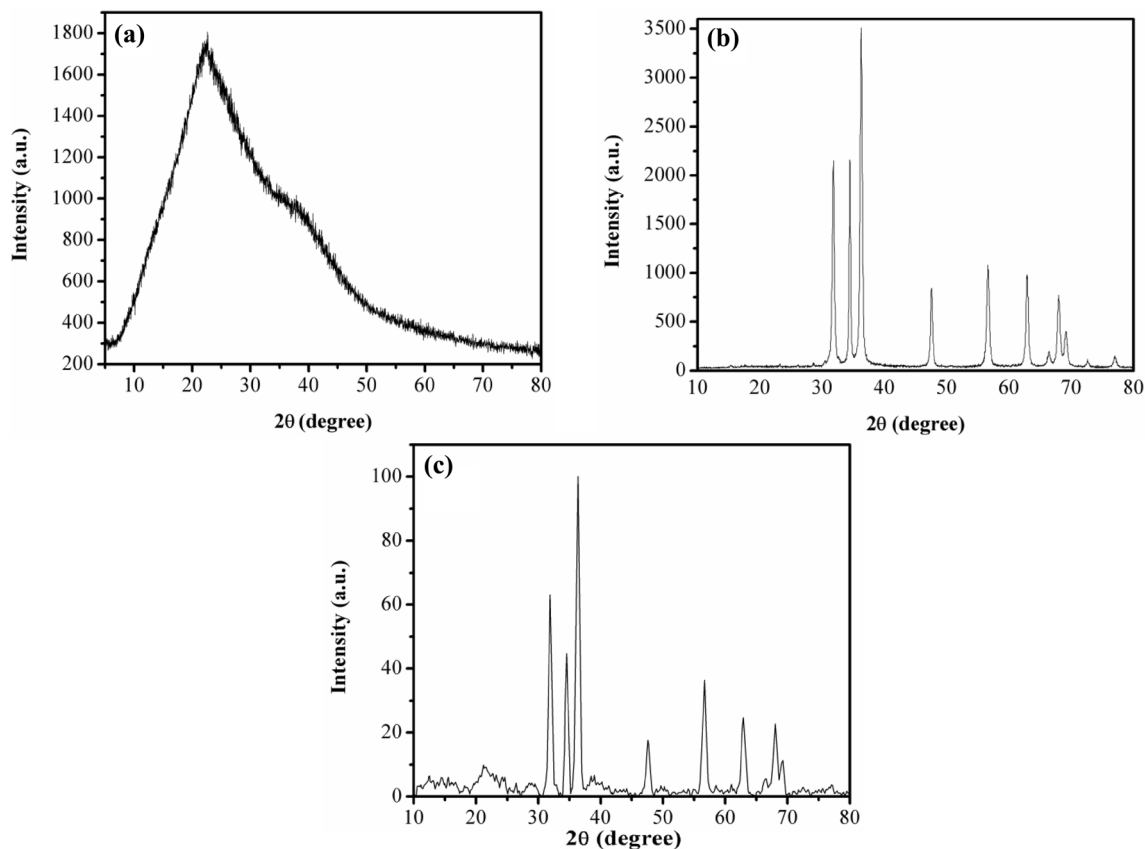


Fig. 4 X-ray diffraction pattern of **a** Pec-g-poly(AMPS-co-AAm), **b** ZnO nanoparticles and **c** Pec-g-poly(AMPS-co-AAm)/ZnO

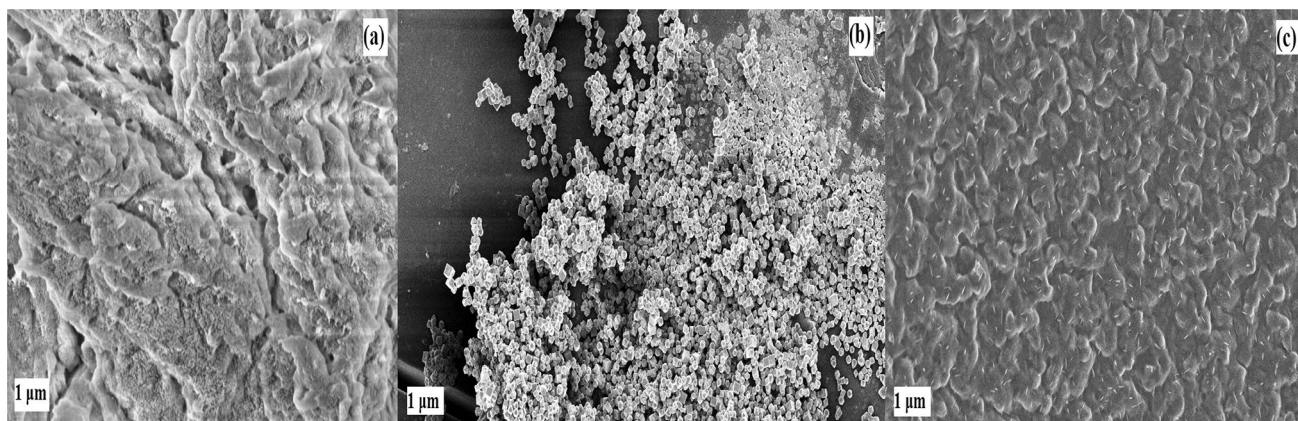


Fig. 5 FESEM images showing the morphology of **a** Pec-g-poly(AMPS-co-AAm), **b** Pec-g-poly(AMPS-co-AAm)/ZnO and **(c)** CV adsorbed Pec-g-poly(AMPS-co-AAm)/ZnO

Swelling Analysis

The swelling behavior of a gel mainly depends on the structure of the network. AMPS has got much attention in swelling studies due to its strongly ionizable sulfonate group which dissociates in the whole pH range [34]. Equilibrium swelling of the hydrogel Pec-g-poy(AMPS-co-AAm) and the nanocomposite

hydrogel Pec-g-poy(AMPS-co-AAm)/ZnO in buffer solutions of pH ranging from 1.2 to 13.0 is shown in Fig. S1 (Supporting information). It is clear from the figure that the maximum swelling is observed in deionized water. This hydrophilicity of the system, Pec-g-poy(AMPS-co-AAm) is due to the presence of carboxylic group ($-\text{COOH}$) and hydroxyl group ($-\text{OH}$) of pectin, sulfonate group ($-\text{SO}_3^-$) of AMPS, amide ($-\text{CONH}-$)

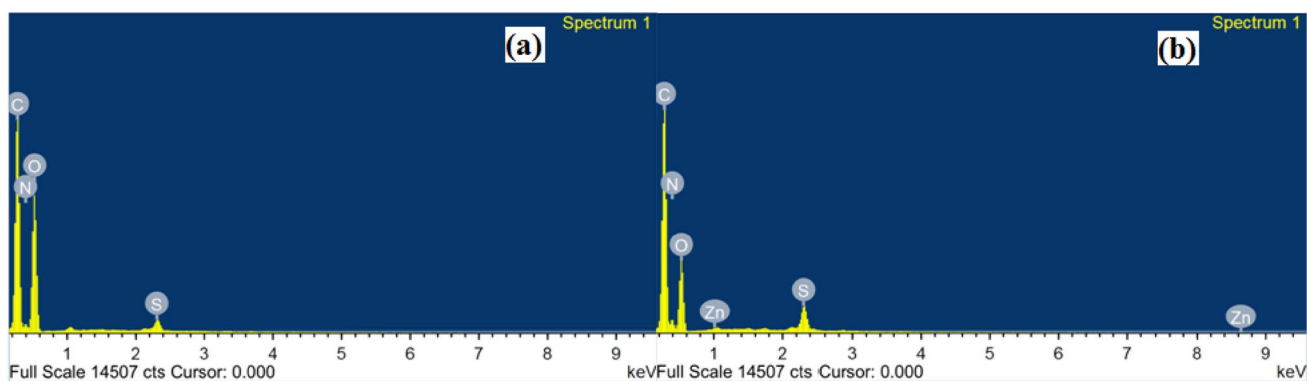


Fig. 6 EDS of **a**) Pec-g-poly(AMPS-co-AAm) and **b**) Pec-g-poly(AMPS-co-AAm)/ZnO

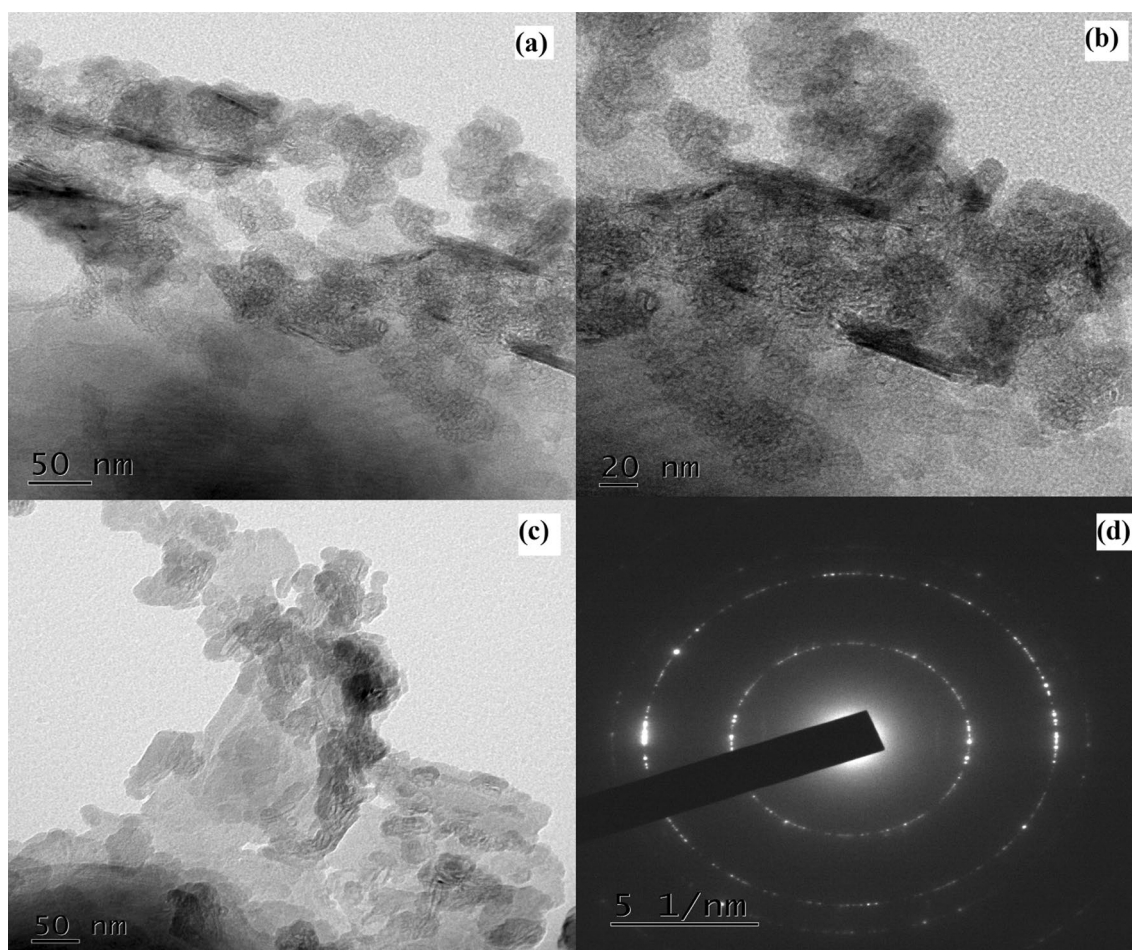


Fig. 7 **a–c** TEM images and **d** selected area electron diffraction (SAED) pattern of ZnO nanoparticles

group of MBA and primary amide ($-\text{CONH}_2$) group of polyacrylamide [49]. In the aqueous medium, the ions are more strongly solvated rather than non-ionic groups [50]. The presence of large number of ionizable groups makes the polymer exhibit pH dependent swelling. As the pH of the medium increases above the pK_a of Pec (3.5), a drastic increase in

swelling is observed. At pH lower than pK_a value, the carboxylic groups of Pec are in undissociated state and the gel exhibits low swelling ratio [42]. At pH values higher than the pK_a value, the swelling ratio increases because of the dissociation of these groups. The sulfonic groups of AMPS ionize fairly easily at all pH. This aids in attracting the polar water

molecules to the sulfonate groups, resulting in the high water absorption capacity of the hydrogel. The acrylamide units being nonionic do not affect swelling. Moreover the hydrogen bonding formed by water molecules with the functional groups of the network also contribute to the increased swelling at neutral pH. In basic medium, screening of charges on the network by electrolytes present in the medium results in the contraction of gel network and the swelling ratio again decreases. In the case of the nanocomposite hydrogel, Pec-g-poy(AMPS-co-AAm)/ZnO the swelling ratio was found to decrease in comparison with the parent hydrogel network. This can be due to the accumulation of hydrophobic nanoparticles within the network system resulting in lowering of hydrogen bonding with water molecules and contraction of network structure.

The kinetic analysis of swelling data has been made and the second order swelling rate constant (K_s) [51] is calculated from the equation.

$$t/SR = \frac{1}{K_s \times (SR_{eq}^2)} + \frac{t}{SR_{eq}} \tag{4}$$

where t is the time in minute, SR is the swelling ratio at time t and SR_{eq} is the equilibrium swelling ratio.

Table 1 Data of equilibrium swelling ratio (SR_{eq}), second order swelling rate constant (K_s) and regression coefficient (R^2) of Pec-g-poly(AMPS-co-AAm) and Pec-g-poly(AMPS-co-AAm)/ZnO nanocomposite hydrogel

System	pH	Parameters		R^2
		SR_{eq} (g/g)	$K_s \times 10^{-3}$ (g/g/min.)	
Pec-g-poly(AMPS-co-AAm)	1.2	13.99	0.95	0.981
	3.0	13.47	1.10	0.964
	7.0	28.12	0.38	0.962
	9.0	18.39	0.63	0.975
	13.0	17.45	0.60	0.968
Pec-g-poly(AMPS-co-AAm)/ZnO	1.2	03.78	6.58	0.999
	3.0	04.73	3.41	0.996
	7.0	16.54	0.93	0.995
	9.0	04.22	4.03	0.996
	13.0	04.45	6.07	0.998

Table 2 Adsorption capacities of Pec-g-(PAMPS-co-PAAm) and Pec-g-(PAMPS-co-PAAm)/ZnO in varying concentrations of CV

C_o (ppm)	20	40	60	80	100	200	300	400	
Pec-g-poly(AMPS-co-AAm)	Q_e (mg/g)	59	109	158	182	214	302	345	363
Pec-g-poly(AMPS-co-AAm)/ZnO		74	134	232	266	327	519	553	579

Weight of the sample: 12 ± 2 mg; contact time: 7 h; temperature: 28 °C; pH: 7.0

The regression coefficient (R^2) values were calculated from the plot of t/SR (time/swelling ratio) vs time are listed in Table 1. From the intercept of the plot the value of second order swelling rate constant (K_s) has been calculated. It is evident that the swelling behavior follows second order kinetics as R^2 values are 0.96 or higher indicating good fit of the data. The swelling data for Pec-g-poy(AMPS-co-AAm) and Pec-g-poy(AMPS-co-AAm)/ZnO in buffer media of varying pH plotted as t/SR vs t are shown in Fig. S2a and S2b (Supporting information) respectively.

Dye Adsorption and Desorption Studies

Adsorption capacity of the nanocomposite hydrogel towards dye molecules has been compared with the parent copolymer gel using CV as the model dye.

Adsorption experiments were carried out in distilled water at room temperature with varying concentration of CV, keeping all other parameters constant. The equilibrium adsorption of CV from different concentrations of dye solutions on Pec-g-poy(AMPS-co-AAm) and Pec-g-poy(AMPS-co-AAm)/ZnO are shown in Table 2. The effect of initial dye concentration on Pec-g-poy(AMPS-co-AAm) and Pec-g-poy(AMPS-co-AAm)/ZnO are displayed in Fig. S3 (Supporting information). The extent of adsorption is found to increase as the dye concentration increases and attains a constant value around 400 mg/L dye concentration. In neutral pH conditions of adsorption, the acidic groups of Pec are deprotonated and results in the electrostatic interaction with the cationic dye molecules. Electrostatic interaction also exists between the strongly ionizable sulfonate groups of AMPS and the cationic dye. In addition to these sites, the porosity of the material also contributes to the adsorption process by entrapping organic dye molecules within the gel network. The ZnO nanoparticles also provide additional sites for the dye molecules to get adsorbed due to their higher surface area. Due to the presence of ZnO nanoparticles, the nanocomposite was found to be more effective in adsorbing CV compared to the parent gel. The possible interactions of CV with the adsorbent are given in Fig. 8.

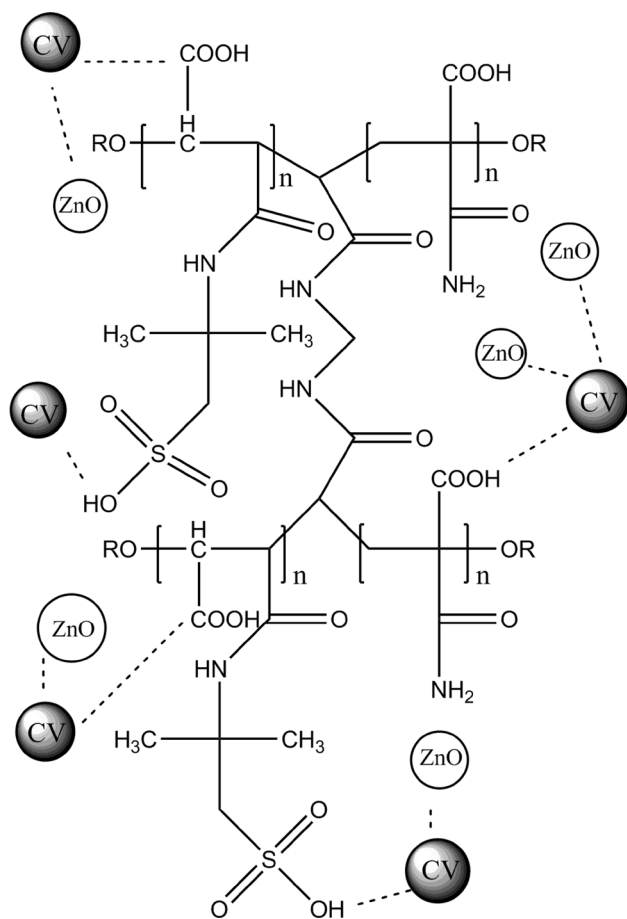


Fig. 8 Possible interaction of CV with the adsorbent material

Adsorption Isotherm Studies

Three types of adsorption isotherm models namely, Freundlich [52], Langmuir [53] and Temkin [54] models have been considered to fit the adsorption data in the present study. The Freundlich isotherm is expressed by the following empirical equation

$$Q_e = K_F C_e^{1/n} \quad (5)$$

The logarithmic form of above equation is

$$\log Q_e = \log K_F + \frac{1}{n} \log C_e \quad (6)$$

where Q_e is the amount of dye adsorbed per unit mass of adsorbent at equilibrium (mg/g), C_e is the concentration of the dye solution at equilibrium (mg/L), K_F and n indicate the extent of the adsorption and the degree of nonlinearity between the solution concentration and the adsorbate respectively and are known as Freundlich adsorption isotherm constants. The values of K_F and n can be calculated from the intercept and slope of the plot between $\log Q_e$ and $\log C_e$

respectively. The adsorption is considered to be favorable only if the value of n lies between 1 and 10.

Langmuir adsorption model makes an assumption that the maximum adsorption corresponds to the formation of saturated monolayer on the surface of adsorbent. The equation representing Langmuir adsorption isotherm is expressed as below

$$\frac{C_e}{Q_e} = \frac{1}{Q_m} C_e + \frac{1}{Q_m K_L} \quad (7)$$

where C_e and Q_e have their usual meaning, Q_m is the maximum amount of adsorbate corresponding to complete monolayer coverage on the adsorbent surface (mg/g), and K_L is the Langmuir constant. The essential characteristics of the Langmuir isotherm, R_L , the separation factor is a dimensionless constant which can be calculated from the following equation [55],

$$R_L = \frac{1}{1 + K_L C_0} \quad (8)$$

where C_0 (mg/L) is the highest initial concentration of adsorbent corresponding to maximum adsorption, and K_L (L/mg) is the Langmuir constant.

The adsorbent-adsorbate interactions can be explained by Temkin isotherm model. It is based on the assumption that the heat of adsorption of all molecules would decrease linearly. The model is mathematically expressed as given in Eq. (9). The constants of Temkin isotherm model were calculated from the intercept and slope of the plot of Q_e vs $\ln C_e$.

$$Q_e = \frac{RT}{b_T} \ln(A_T C_e) \quad (9)$$

where Q_e and C_e are as defined earlier. R is universal gas constant (8.314 J/mol/K), b_T is Temkin isotherm constant and A_T is Temkin isotherm equilibrium bridging constant (L/g) and T is the temperature in Kelvin.

The value $\frac{RT}{b_T}$ is a constant which is related to heat of sorption and is represented by B .

The adsorption data obtained in the present study, plotted as per Eqs. (6), (7) and (9) are shown in Fig. 9. The constants R_L , K_L , Q_m , K_F , n , b_T , A_T and B determined from the intercepts and slopes of the linear plots are presented in Table 3.

The obtained R_L values indicate that the adsorption of crystal violet on both Pec-g-poy(AMPS-co-AAm) and Pec-g-poy(AMPS-co-AAm)/ZnO is favorable, the value of Q_m for both the systems are found to be almost equal to that of experimental Q_e values and the R^2 values of 0.999 and 0.996 for Langmuir model fit strongly supports that the adsorption of CV follows the Langmuir isotherm model. This indicates that the adsorption process is due to the weak interaction between the adsorbent and the adsorbate resulting in

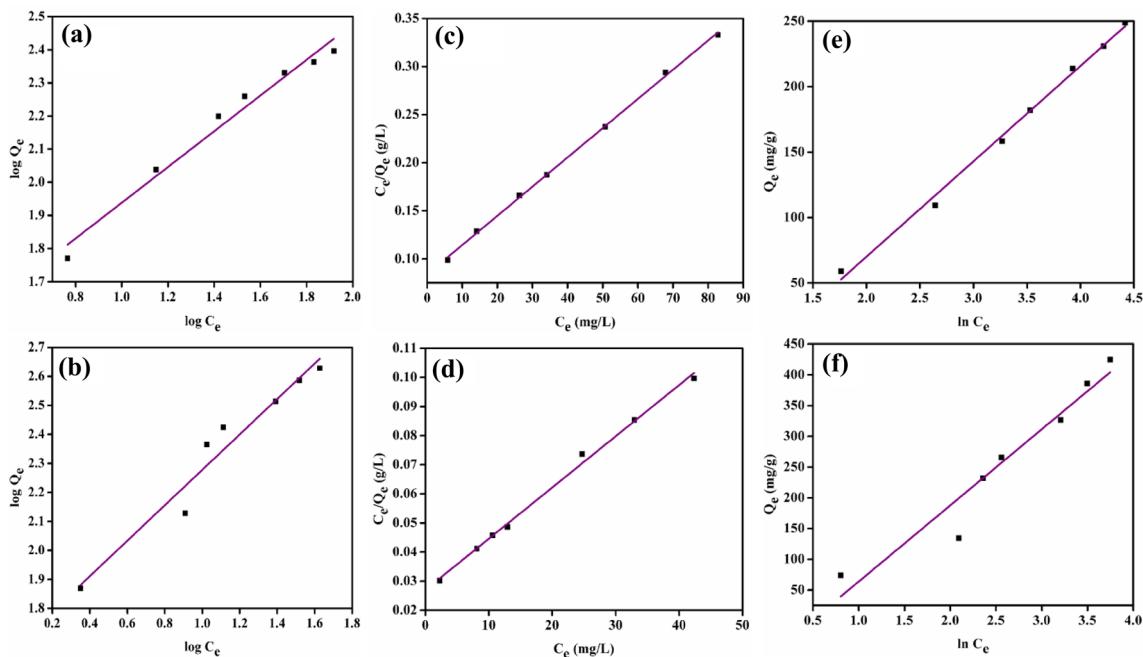


Fig. 9 a, b Freundlich, c, d Langmuir and e, f Temkin plot for the adsorption of CV on Pec-g-poly(AMPS-co-AAm) and Pec-g-poly(AMPS-co-AAm)/ZnO respectively

physical interaction leading to the monolayer saturation on the adsorbent material.

Adsorption Kinetic Studies

Two models have been used for the investigation of kinetics of dye adsorption, namely, the Lagergren ‘pseudo-first-order model’ [53] and the Ho ‘pseudo-second order model’ [56].

The Lagergren ‘Pseudo-First-Order Model’ It is based on the assumption that the rate of change of adsorbate uptake over time is directly proportional to the difference in saturation concentration and the amount of adsorbate uptake over time. The mathematical representation of pseudo first order kinetics is:

$$\frac{dQ_t}{dt} = k_1(Q_e - Q_t) \tag{10}$$

Integrating the above equation and noting that $Q_t=0$ when $t=0$, we get;

$$\log(Q_e - Q_t) = \log Q_e - \frac{k_1 t}{2.303} \tag{11}$$

where Q_e is the amount of dye adsorbed at equilibrium, Q_t is the amount of dye adsorbed per unit of adsorbent (mg/g) at time t , k_1 is the pseudo-first-order rate constant (min^{-1}), and t is the contact time (min). The Q_e and k_1 values are calculated from the intercept and slope of the plot of $\log(Q_e - Q_t)$ vs t (not shown) are given in Table 4.

The Ho ‘Pseudo-Second Order Model’ The Ho ‘pseudo-second order can be represented by the equation

$$\frac{dQ_t}{dt} = k_1(Q_e - Q_t)^2 \tag{12}$$

On integrating the above equation with boundary conditions, $Q_t=0$ at $t=0$, we get,

Table 3 Adsorption isotherm parameters for the adsorption of CV on Pec-g-poly(AMPS-co-AAm) and Pec-g-poly(AMPS-co-AAm)/ZnO

Isotherm models	Parameters	Adsorbate	
		Pec-g-poly(AMPS-co-AAm)	Pec-g-poly(AMPS-co-AAm)/ZnO
	Q_e (mg/g), calculated	362.62	579.18
Freundlich	K_F	25.10	46.43
	n	1.86	1.64
	R^2	0.977	0.951
Langmuir	R_L	0.165	0.099
	K_L	0.036	0.065
	Q_m (mg/g)	329.08	568.33
	R^2	0.999	0.996
Temkin	B (J/mol)	72.85	123.88
	A_T (L/g)	0.354	0.616
	b_T	34.01	20.00
	R^2	0.995	0.937

Table 4 Pseudo first order and pseudo second order kinetic parameters for the adsorption process

	Adsorbate		
	Pec-g-poly(AMPS-co-AAm)	Pec-g-poly(AMPS-co-AAm)/ZnO	
Concentration (C_0) (mg/L)	100	100	
Q_e (experimental) (mg/g)	222.86	352.16	
Kinetic model			
Pseudo-first order	Q_e (mg/g)	17.27	12.99
	k_1 (min^{-1})	0.0062	0.0049
	R^2	0.638	0.457
Pseudo-second order	Q_e (mg/g)	222.22	351.13
	k_2 (g/mg/min)	0.0020	0.0023
	h (mg/g/min)	98.95	281.79
	R^2	0.999	0.999

$$\frac{t}{Q_t} = \frac{1}{k_2 Q_e^2} + \frac{t}{Q_e} \quad (13)$$

where k_2 is the pseudo-second order rate constant (g/mg/min). The initial adsorption rate, h is defined as

$$h = k_2 Q_e^2 \quad (14)$$

The values of Q_e , k_2 and h obtained from the linear plot of t/Q_t vs t (Fig. 10) are given in Table 4. The adsorption process follows pseudo-second order model since the highest value of regression coefficient (R^2) is obtained for this model as reported in earlier studies [57, 58]. The Q_e value obtained from the calculation is closer to the experimental value. Also the initial adsorption rate of the system was found to be high indicating the rapid accumulation of adsorbate molecules on the adsorbent system. The initial rate of adsorption is

found to be three times higher in case of nanocomposite sample when compared to the parent gel which indicates the influence of ZnO nanoparticles on rate of adsorption. Hence it can be said that the adsorption of CV on Pec-g-poy(AMPS-co-AAm) and Pec-g-poy(AMPS-co-AAm)/ZnO follows pseudo-second order kinetics rather than pseudo-first order kinetics.

Thermodynamic Parameters

The thermodynamic parameters such as changes in standard free energy (ΔG°), enthalpy (ΔH°) and entropy (ΔS°) associated with adsorption process were calculated from the following equations

$$\Delta G^\circ = -RT \ln K_c \quad (15)$$

$$\Delta G^\circ = \Delta H^\circ - T\Delta S^\circ \quad (16)$$

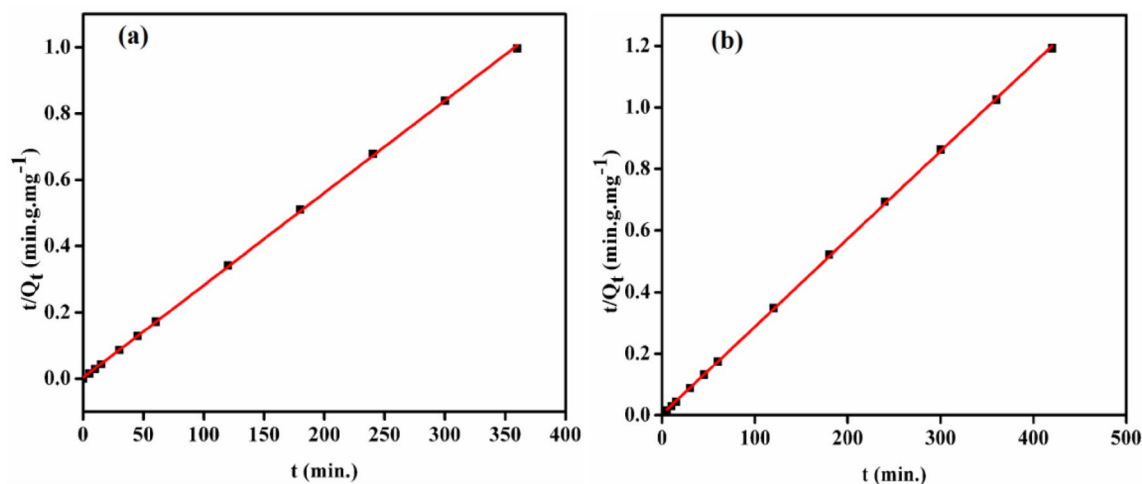
where K_c is the equilibrium constant of adsorption and it can be obtained from the equation

$$K_c = \frac{Q_e}{C_e} \quad (17)$$

The combination of Eqs. (15) and (16) gives the van't Hoff equation, which is written as

$$\ln K_c = \frac{-\Delta H^\circ}{R} \frac{1}{T} + \frac{\Delta S^\circ}{R} \quad (18)$$

ΔH° and ΔS° were calculated from the slope and intercept of the plot of $\ln K_c$ vs $1/T$ (Fig. S4; Supporting information). Values of $\ln K_c$, ΔG° , ΔH° and ΔS° are listed in Table 5. The negative value of ΔS° indicates the decreased randomness during the adsorption process. ΔH° value obtained is negative and it suggests the adsorption process to be exothermic in nature. A decrease in ΔG° as the temperature increases

**Fig. 10** Pseudo-second order plot for the adsorption of CV on **a** Pec-g-poly(AMPS-co-AAm) and **b** Pec-g-poly(AMPS-co-AAm)/ZnO

was observed and it indicates the spontaneity of adsorption on Pec-g-poy(AMPS-co-AAm) and Pec-g-poy(AMPS-co-AAm)/ZnO [22].

Desorption Experiments

Aqueous solution of pH 1.2 (prepared using concentrated hydrochloric acid) was used as the stripping solution since Pec-g-poy(AMPS-co-AAm) and Pec-g-poy(AMPS-co-AAm)/ZnO have low affinity for CV molecules at acidic pH. At acidic pH the carboxylic groups of pectin get protonated due to their high affinity towards acidic proton and result in weak interaction with the cationic dye. The dye molecules thus get released to the acidic media. The results of adsorption and desorption experiments are shown in Table 6. Around 96% of CV could be desorbed to the stripping solution over a time period of 2 h which supports the repeated use of presently synthesized materials as adsorbents towards cationic dyes.

Comparison of the Adsorption Efficiency of the Nanocomposite Hydrogel with Other Adsorbents

The adsorption data of the presently studied gel samples for CV was compared with some reported adsorbents and listed in Table 7. Monash et al. [59] reported the use of uncalcined ball clay for the adsorption process which describes a low level adsorption of CV from an acidic medium. Dual physically cross linked hydrogels containing laponite clay [60], magnetite/pectin and magnetite/silica/pectin hybrid nanocomposite [30], poly(4-styrenesulfonic acid-co-maleic acid) sodium modified magnetic reduced graphene oxide nanocomposites [61], vitreous tuff mineral [62], magnetic Fe₃O₄@SiO₂ starch-graft-poly(acrylic acid) nanocomposite hydrogels [63], H₂SO₄ and ZnCl₂ activated rice husk [64] etc. have been reported with good adsorption capacity for the removal of CV from neutral pH solutions. Copper coordination polymer with dithioamide, a metal organic polymer framework [19] has been reported with a maximum of 165.83 mg/g adsorption capacity from acidic pH conditions. When reduced graphene oxide modified with poly(4-styrenesulfonic acid-co-maleic acid) sodium [61], the resulting compound showed much higher

Table 5 Thermodynamic parameters of adsorption of CV on Pec-g-poly(AMPS-co-AAm) and Pec-g-poly(AMPS-co-AAm)/ZnO

Adsorbate	−ΔH° (kJ/mol)	−ΔS° (kJ/mol/K)	−ΔG° (kJ/mol)			
			303 K	308 K	313 K	318 K
Pec-g-poly(AMPS-co-AAm)	72.66	0.2237	4.87	3.71	2.70	1.47
Pec-g-poly(AMPS-co-AAm)/ZnO	66.33	0.1978	6.53	5.26	4.40	3.53

Table 6 Amount of dye molecules adsorbed, desorbed and the percentage of desorption

Adsorbent	Amount of dye adsorbed (mg)	Amount of dye desorbed (mg)	% Desorption
Pec-g-poly(AMPS-co-AAm)	213.8	205.4	96.1
Pec-g-poly(AMPS-co-AAm)/ZnO	326.5	312.5	95.7

Table 7 Comparison of the adsorption capacity of the hydrogel and the nanocomposite hydrogel with other reported adsorbents for the adsorption of CV

Adsorbents	Q _e (mg/g)	pH	Isotherm	Kinetic model	References
UNCAL Ball clay	00.049	5.86	Langmuir and Redlich-Peterson		[62]
DPC gels	95.736	07.0		Pseudo-2nd order	[63]
PAAm-Kaolin	030.30	10.0	Langmuir and Freundlich	Pseudo-2nd order	[17]
M-rGO-060	384.60	07.0	Langmuir	Pseudo-2nd order	[64]
Vitreous tuff	174.01	07.0	Freundlich	Pseudo-2nd order	[65]
Mag./pectin NPs	100.00	07.0	Langmuir	Pseudo-2nd order	[30]
Mag./silica/pectin NPs	125.00	07.0	Langmuir	Pseudo-2nd order	[30]
H2dtoaCu	165.83	11.0	Langmuir	Pseudo-2nd order	[19]
Pec-g-poly(AMPS-co-AAm)	329.08	07.0	Langmuir	Pseudo-2nd order	Present work
Pec-g-poly(AMPS-co-AAm)/ZnO	568.33	07.0	Langmuir	Pseudo-2nd order	Present work

adsorption capacity which is comparable with the present study. Zhou et al. [65] reported the use of cellulose and glycidyl methacrylate and sulfosalicylic acid modified cellulose for the adsorptive removal of CV from basic media. The adsorption capacity of modified cellulose was found to be much higher in comparison with the native cellulose. The gel samples developed in the present work with the incorporation of zinc oxide nanoparticles to the pectin based hydrogel has shown a maximum adsorption capacity of 568.33 mg/g compared to all other samples.

Conclusions

Here in this study we investigated the potential use of a pectin-based graft copolymer, Pec-*g*-poy(AMPS-*co*-AAm) and its nanocomposite with ZnO, Pec-*g*-poy(AMPS-*co*-AAm)/ZnO as adsorbents for cationic dyes such as CV. Swelling studies of the systems under different pH conditions indicated a maximum swelling capacity in neutral pH for both the samples and the nanocomposite having lower swelling compared to the parent gel. The equilibrium swelling of the parent gel was found to be 28.12 g/g whereas that of nanocomposite was 16.54 g/g. The reduction in equilibrium swelling capacity of the nanocomposite has been attributed to the filling of the pores of hydrogel with the ZnO nanoparticles. The dye removal efficiency for the parent gel and the nanocomposite was found to be 329 and 568 mg/g respectively at room temperature. The initial rate of adsorption of the nanocomposite was found to be 281.79 mg/g/min which is three times greater than that of the parent gel (98.95 mg/g/min) indicating the effectiveness in adsorption due to the presence of ZnO nanoparticles. The adsorption equilibrium data was found to fit well with Langmuir model and adsorption was found to be a pseudo-second order process. Evaluation of thermodynamic parameters of the adsorption process indicated the adsorption process to be exothermic and spontaneous. The negative value of ΔG° indicated the adsorption process to be spontaneous at all the studied temperatures. About 96% of adsorbed dye could be desorbed from the gel samples indicating the reusability of gels as adsorbent materials. Therefore, the present study supports the use of the gel Pec-*g*-poy(AMPS-*co*-AAm) and the nanocomposite Pec-*g*-poy(AMPS-*co*-AAm)/ZnO as potential adsorbent materials for the adsorption of cationic dyes from aqueous solutions originating from the industrial effluents.

Data Availability All data generated or analyzed during this study are included in this published article [and its supplementary information files].

Compliance with Ethical Standards

Conflict of interest The authors declare no competing financial interest.

References

- Mohan D, Singh KP, Singh G, Kumar K (2002) *Ind Eng Chem Res* 41:3688–3695
- Lavanya C, Dhankar R, Chhikara S, Sheoran S (2014) *Int J Curr Microbiol Appl Sci* 3:189–199
- Mathur N, Bhatnagar P, Sharma P (2012) *Univ J Environ* 2:1–18
- Ding Y, Sun C, Xu X (2009) *Eur J Mass Spectrom* 15:705–713
- Pathania D, Sharma G, Kumar A, Naushad M, Kalia S, Sharma A, Allothman ZA (2015) *Toxicol Environ Chem* 97:526–537
- Naushad M, Allothman ZA, Awual MR, Alfadul SM, Ahamad T (2016) *Desalin Water Treat* 57:13527–13533
- Ratna, Padhi BS (2012) *Int J Environ Sci* 3:940–955
- de Lima ROA, Bazo AP, Salvadori DMF, Rech CM, Oliveira DP, Umbuzeiro GA (2007) *Mutat Res* 626:53–60
- Albadarin AB, Collins MN, Naushad M, Shirazian S, Walker G, Mangwandi C (2017) *Chem Eng J* 307:264–272
- Salgueiro AM, Daniel-da-Silva AL, Girao AV, Pinheiro PC, Trindade T (2013) *Chem Eng J* 229:276–284
- Xie X, Li X, Luo H, Lu H, Chen F, Li W (2016) *J Phys Chem B* 120:4131–4142
- Mahanta D, Madras G, Radhakrishnan S, Patil S (2009) *J Phys Chem B* 113:2293–2299
- Sharma G, Thakur B, Naushad M, Kumar A, Stadler FJ, Alfadul SM, Mola GT (2018) *Environ Chem Lett* 16:113–146
- Zhou C, Wua Q, Lei T, Negulescu II (2014) *Chem Eng J* 251:17–24
- Kasgoz H, Durmus A (2008) *Polym Adv Technol* 19:838–845
- Bhattacharyya R, Ray SK (2015) *Chem Eng J* 260:269–283
- Shirsath SR, Patil AP, Bhanvase BA, Sonawane SH (2015) *J Environ Chem Eng* 3:1152–1162
- Bharathi KS, Ramesh ST (2013) *Appl Water Sci* 3:773–790
- Li X, Zheng L, Huang L, Zheng O, Lin Z, Guo L, Qiu B, Chen G (2013) *J Appl Polym Sci* 129:2857–2864
- Leung WH, Lo WH, Chan PH (2015) *RSC Adv* 5:90022–90030
- Zhang W, Yang H, Dong L, Yan H, Li H, Jiang Z, Kan X, Li A, Cheng R (2012) *Carbohydr Polym* 90:887–893
- Kumar N, Mittal H, Parashar V, Ray SS, Ngila JC (2016) *RSC Adv* 6:21929–21939
- Ghaedi M, Ansari MA, Habibi MH, Asghari AR (2014) *J Ind Eng Chem* 20:17–28
- Zhang L, Li L, Sun X, Liu P, Yang D, Zhao X (2016) *Materials* 9:927–942
- Zhang W, Zhou Z (2017) *Nanomaterials* 7:1–6
- Gupta VK, Pathania D, Singh P (2014) *Int J Environ Sci Technol* 11:2015–2024
- Sharma G, Naushad M, Pathania D, Kumar A (2016) *Desalin Water Treat* 57:19443–19455
- Singha NR, Karmakar M, Mahapatra M, Mondal H, Dutta A, Roy C, Chattopadhyay PK (2017) *Polym Chem* 8:3211–3237
- Sharma G, Naushad M, Pathania D, Mittal A, El-desoky GE (2015) *Desalin Water Treat* 54:3114–3121
- Attallah OA, Al-Ghobashy MA, Nebsen M, Salem MY (2016) *RSC Adv* 6:11461–11480
- Naushad M, Sharma G, Kumar A, Sharma S, Ghfar AA, Bhatnagar A, Stadler FJ, Khan MR (2018) *Int J Biol Macromol* 106:1–10
- Rakhshae R, Panahandeh M (2011) *J Hazard Mater* 189:158–166

33. Mishra RK, Datt M, Bantia AK (2008) *AAPS PharmSciTech* 9:395–403
34. Durmaz S, Okay O (2000) *Polymer* 41:3693–3704
35. Khosla E, Kaur S, Dave PN (2015) *Chem Ecol* 31:173–185
36. Kulkarni AV, Chavhan A, Bappakhane A, Chimmankar J (2016) *Res J Chem Environ Sci* 4:158–163
37. Khoshhesab ZM, Gonbadi K, Behbehani GR (2015) *Desalin Water Treat* 56:1558–1565
38. Morsi RE, Elsalamony RA (2016) *New J Chem* 40:2927–2934
39. Salehi R, Arami M, Mahmoodi NM, Bahrami H, Khorramfar S (2010) *Colloids Surf B* 80:86–93
40. Sani HA, Aliyu HS, Tukur SA (2015) *IOSR JAC* 8:34–38
41. Arafat A, Samad SA, Huq D, Moniruzzaman M, Masum SM (2015) *J Tex Sci Eng* 5:1–4
42. Tian Q, Wu W, Yang S, Liu J, Yao W, Ren F, Jiang C (2017) *Nanoscale Res Lett* 12:1–10
43. Kumar SS, Venkateswarlu P, Rao VR, Rao GN (2013) *Int Nano Lett* 3:1–6
44. Krishna KA, Vishalakshi B (2017) *Elixir Nanotechnology* 107:47326–47331
45. Kodoth AK, Ghate VM, Lewis SA, Badalamoole V (2018) *Int J Biol Macromol* 115:418–430
46. Kodoth AK, Badalamoole V (2019) *Polym Bull.* <https://doi.org/10.1007/s00289-019-02757-4>
47. Naushad M, Ahamad T, Sharma G, Al-Muhtaseb AH, Albadarin AB, Alam MM, Allothman ZA, Alshehri SM, Ghfar AA (2016) *Chem Eng J* 300:306–316
48. Voicu G, Oprea O, Vasile BS, Andronescu E (2013) *Dig J Nanomater Biostruct* 8:667–675
49. Ganji F, Farahani SV, Farahani EV (2010) *Iran Polym J* 19:375–398
50. Kazemzadeh B, Hosseinzadeh H, Babazadeh M (2013) *Biomed Pharm J* 6:41–48
51. Pourjavadi A, Mahdavinia GR (2006) *Turk J Chem* 30:595–608
52. Gueu S, Yao B, Adouby K, Ado G (2007) *Int J Environ Sci Technol* 4:11–17
53. Langmuir I (1918) *J Am Chem Soc* 40:1361–1403
54. Dada AO, Olalekan AP, Olatunya AM, Dada O (2012) *IOSR JAC* 3:38–45
55. Hall KR, Eagleton LC, Acrivos A, Vermeulen T (1966) *Ind Eng Chem Fundam* 5:212–223
56. Ho YS, McKay G (1999) *Process Biochem* 34:451–465
57. Naushad M, Allothman ZA, Sharma G (2015) *Inamuddin. Ionics* 21:1453–1459
58. Alqadami AA, Naushad M, Allothman ZA, Ghfar AA (2017) *ACS Appl Mater Interfaces* 9:36026–36037
59. Monash P, Niwas R, Pugazhenth G (2011) *Clean Technol Environ* 13:141–151
60. Cui W, Zhang Z, Li H, Zhu L, Liua H, Ran R (2015) *RSC Adv* 5:52966–52977
61. Song Y, Song X, Cheng C, Zhao Z (2015) *RSC Adv* 5:87030–87042
62. Flores AB, Cruz AC, Segura EG, Mendieta VS, Casados DAS, Guirado MAG, Gonzalez RB (2014) *Environ Technol* 35:1508–1519
63. Pourjavadi A, Hosseini SH, Seidi F (2012) *Rouhollah. Polym Int* 62:1038–1044
64. Mohanty K, Naidu JT, Meikap BC, Biswas MN (2006) *Ind Eng Chem Res* 45:5165–5171
65. Zhou Y, Zhang M, Wang X, Huang Q, Min Y, Ma T, Niu J (2014) *Ind Eng Chem Res* 53:5498–5506

Publisher's Note Springer Nature remains neutral with regard to jurisdictional claims in published maps and institutional affiliations.